Nanolime deposition in Maastricht limestone: back-migration or accumulation at the absorption surface?

G. Borsoi[a], R. van Hees[b], B. Lubelli[b], R. Veiga[c], A. Santos Silva[c]

[a] Heritage & Architecture Section, Faculty of Architecture, Delft University of Technology, Delft, The Netherlands

[b] Division of Structural Reliability, TNO, Delft, The Netherlands

[c] Building Division and Material Division, National Laboratory of Civil Engineering - LNEC, Lisbon, Portugal

* G.Borsoi@tudelft.nl

Abstract

The development of nanomaterials is growing exponentially in the last decade. New discoveries and their applications have taken place in different fields, such as electronics, chemistry, biology and physics. Some innovative nanoproducts have become available also for the conservation of cultural heritage (e.g. nano-$Ca(OH)_2$, nano-SiO_2, nano-TiO_2, CNTs, etc.), showing interesting potentialities and advantages. However, there are also drawbacks.

Extensive literature is available on nanolimes, i.e. colloidal alcoholic dispersions of $Ca(OH)_2$ nanoparticles, which are promising materials for the consolidation of lime-based plasters and calcareous stone, often present in ancient masonry structures. Nanolimes have several advantages such as high stability, fast carbonation rate and good chemical and physical compatibility with calcareous stone and lime-based plasters. However, in comparison to other existing consolidant products, like TEOS-based (Tetraethylorthosilicate), the penetration depth of nanolime is often limited, which may consequently result in a low effectiveness.

The research presented in this paper aimed at understanding the penetration and deposition process of nanolime when applied in Maastricht limestone, a soft, highly porous substrate, widely used in the Dutch and Belgian provinces of Limburg. This research focused on the nanolime transport process to clarify whether nanolime is able to penetrate and deposit in depth in the material or if it simply accumulates near the surface. In order to investigate the distribution and particle size of nanolime deposited in the stone, next to simple phenolphthalein tests, optical microscopy, AFM and SEM-EDS were used. On the basis of the obtained results, the transport and deposition of a commercial nanolime in Maastricht limestone has been elucidated. The comprehension of the nanolime transport mechanism (penetration and distribution) within the treated material is crucial for improving the effectiveness of this consolidation treatment.

Keywords: Nanolime, Consolidation products, Transport, Penetration depth, Limestone

I. Introduction

Calcareous stone (e.g. limestone) and lime-based finishes (e.g. renders, plasters and mural painting) are often subjected to several degradation processes (e.g. salt crystallization, frost action, biological growth); these factors that can lead to decay patterns i.e. powdering, sanding, scaling or chalking (Figure 1a,b).

Interventions on these kinds of historical substrates anyway differ significantly; different theoretical approaches and practical recommendations are found in the European context. A restoration, meant recover the loss of cohesion of materials, can include pre-consolidation (to avoid material loss in the following phases), cleaning (e.g. by poultice methods or laser ablation) and desalination (e.g. with poultice methods).

These processes are generally followed by the application of a consolidant, which can recover the lost cohesion; consolidation can easily stabilize superficial decay forms as powdering, sanding and chalking; pathologies as exfoliation, scaling or flaking can generally not be treated.

Consolidants are usually applied to stone, renders or plasters by brush, spray or by immersion and penetrate into the treated material by capillary action (Doehne 2010). Anyway the application of a consolidant is a physically irreversible treatment and is therefore a critical treatment that has to be properly studied and well conceived. Consolidation is in fact a risky operation and it is not difficult to find situations where consolidation has left a negative imprint and serious drawbacks (Delgado 2010).

A consolidation treatment should guarantee three fundamental requirements: effectiveness (i.e. improvement of the mechanical strength) compatibil-

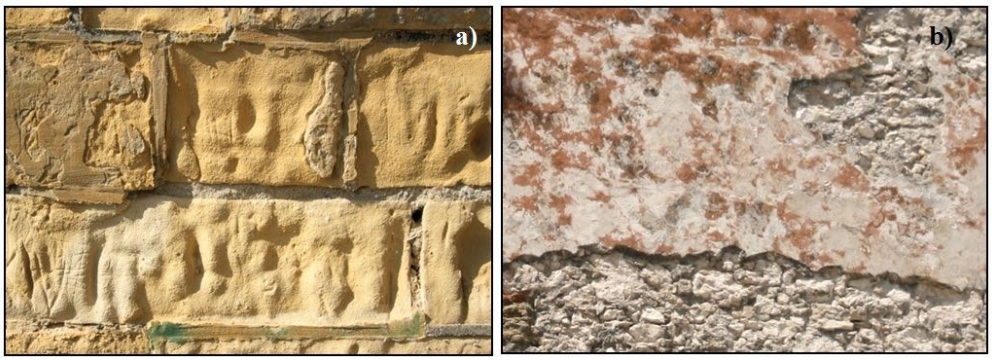

Figure 1: (a) Loss of cohesion, powdering and traces of past interventions are visible in this masonry of Maastricht Limestone (Keverborg castle, Kessel, The Netherlands); b) detachment, loss of cohesion and material in coloured lime-based mortars applied on historical stone masonry (Alcantâra Convent, Lisbon, Portugal)

ity (with the treated substrate) and long term durability (resistance to different damage mechanisms) (Hansen, 2003; Toniolo, 2010; Van Hees, 2014). The concept of *compatibility* of an intervention has nowadays replaced that of reversibility (Teutonico, 1997; Van Hees, 2014). Products used for conservation issues should be compatible, from the mechanical, chemical physical and aesthetical point of view, with the substrate on which they are applied.

Inorganic lime-based consolidants are in theory more suitable for limestone than the organic ones (as TEOS-based consolidants), because of their better compatibility [Doehne 2010]. The historically most known inorganic lime-based consolidant product is limewater, a $Ca(OH)_2$ aqueous solution. Limewater, however, has a poor penetration depth and effectiveness, because of the low solubility of calcium in water.

Alternatives to limewater have been explored over the last decade, as the use of alcoholic dispersions of calcium hydroxide nanoparticles, commonly known as *nanolimes* (Giorgi, 2000; Dei, 2006). Nanolimes are colloidal alcoholic dispersions with high stability and high lime concentration, facts that in theory would improve the consolidating action (Chelazzi, 2013; Ziegenbalg, 2010). Nanolimes are usually synthesized under controlled conditions by homogeneous phase reaction (Salvadori, 2001; Dei, 2006) or solvothermical reaction (Favaro, 2008; Ziegenbalg, 2010; Poggi, 2012). Calcium hydroxide nanoparticles have a size between 50 and 600 nm.

This lime-based colloidal dispersion has been applied in conservation for the pre-consolidation and for the recovery of the superficial cohesion (Ambrosi, 2001; Dei, 2006; Poggi, 2012; Borsoi, 2012; Baglioni, 2013; Chelazzi, 2013; Rodriguez-Navarro, 2013, Carretti, 2014). However, when mass consolidation is required, as in the case of render or stone, the potential of nanolimes is still questioned (Campbell, 2010; Hull, 2012). One of the reasons of the limited effectiveness of these products is the accumulation of nanolime at or just beneath the drying surface (often with the formation of a white patina) (Ghaffari, 2012; Costa, 2011).

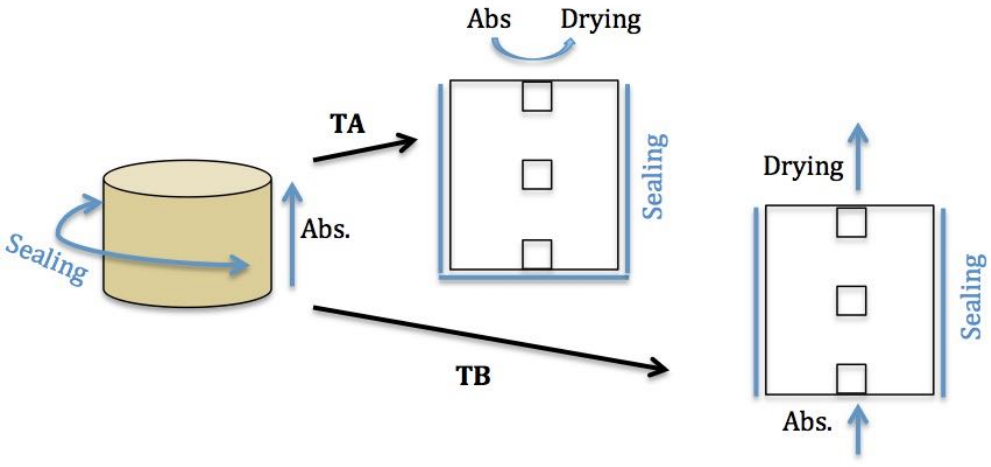

Figure 2: Specimen set up and relative sampling spots; TA: absorption and drying perferomed on the same side; TB: absorption on one side (then sealed), drying on the opposite side.

In order to improve the consolidation effect in depth, the transport mechanism and the deposition of nanolimes within porous materials, as stone or renders, should be better understood. Nanolime transport mechanism has not been systematically studied yet. Does nanolime accumulate at the surface during absorption or is it able to penetrate in depth in the material, but it migrates back to the surface during the drying process? What is the role of nanolime stability and nanoparticles aggregation phenomena in nanolime deposition in a treated material?

This research aimed at clarifying the transport and deposition mechanisms of nanolime in porous materials. The transport of a commercial nanolime product was studied on Maastricht limestone, a high porosity yellowish limestone. The absorption and drying behaviour of nanolime was measured and compared to that of ethanol (the dispersant of this nanolime commercial product) and water (section 3.2). Next to simple phenolphthalein tests on cross sections (section 3.3), microscopy observations by AFM (section 3.1), optical microscopy (3.4) and SEM-EDS (3.5) were performed; the purpose is to investigate nanolime penetration depth and deposition within the material as result of the transport mechanism.

II. Materials and methods

Substrate

The Maastricht limestone is an almost pure calcareous building material (≈95% $CaCO_3$) (Nijland, 2006), quarried in the Belgian and Dutch provinces of Limburg (Dubelaar, 2006). It has high porosity (45-50%) and unimodal pore distribution (35-40 μm). Those characteristics, combined with a weak cementation, lead to some unbelief with respect to its use as a major good-quality building stone (Dreesen, 2004).

A large number of historical buildings have indeed been built almost exclusively with this material and have remained rather unaffected after centuries of environmental exposure (Dreesen, 2004; Van Hees, 2009). Its durability is possibly linked to the dissolution and re-precipitation of carbonates within the limestone pores network, when exposed to atmospheric agents (Dusar, 2003). This process was traditionally enhanced by the application of limewater (*kalkwei*), which forms a sort of durable protective layer (Dreesen, 2004). Despite its good durability, this material may in some cases show decay in the form of loss of cohesion of the surface (Figure 1a) (Nijland, 2006).

Nanolime

The commercial nanolime *CaloSil E25* (IBZ, Germany), reported in the text just as *E25*, has been tested. This colloidal dispersion has a calcium hydroxide nanoparticles concentration of 25 g/l and is dispersed in ethanol. E25 is obtained by solvothermical reaction of metallic calcium in water or alcohols (e.g. ethanol, propanol, isopropanol). Nanoparticles have hexagonal plate-like shape and size ranges between 50 and 250 nm (Ziegenbalg, 2010). Before use, E25 was placed in an ultrasonic bath (60 Hz) for 10 minutes, to minimize nanoparticle aggregation phenomena. Ethanol (p.a. >99.5%, by Sigma Aldrich) and distilled water (conductivity $< 2\ \mu$s/cm) were used for comparison with the E25.

Absorption and drying tests

Maastricht limestone core specimens (4 cm height, 4 cm diameter), drilled from sound blocks, were used for the capillary absorption and drying measurements. The capillary absorption and drying were measured for E25 as well as for ethanol and water.

The specimens were sealed on the lateral side with parafilm in order to prevent evaporation on these sides. The capillary absorption was measured by partially immersing the specimens in a petri dish, filled with nanolime, ethanol or water. The weight of the core specimens was measured at regular intervals during the absorption process till saturation was reached, and the height of the wetting front was monitored and photographically recorded. Water, ethanol and nanolimes absorption were carried out in sequence on the same specimens, in order to minimize the effect of the stone variability.

The drying behavior of specimens saturated with nanolime, ethanol and water was evaluated by measuring the weight loss over time. Both absorption and drying measurements were performed in threefold and under controlled conditions (50% RH, T=20 °C, air speed $<$ 0,1 m/s).

Additionally, in the case of nanolime, in order to clarify if any nanolime accumulation at the absorption surface occurs during absorption or drying, the absorption and drying were repeated according to two different test procedures, as shown in Figure 2. In one case (specimen *TA*), the drying was performed on the same side of the absorption (as it normally occurs in the practice of conservation); in the other case (specimen *TB*) the drying was performed through the surface opposite to the absorption surface (which was sealed after specimen saturation with nanolime).

Phenolphthalein test

The penetration of the lime nanoparticles immediately after absorption was assessed by phenolphthalein test. After complete saturation, the cross section of the specimen was nebulized with a 1% phenolphthalein solution in ethanol and water. Phenolphthalein is a pH indicator that turns purple when pH conditions are higher than 9,8. In this case a purple color of the substrate, treated with phenolphthalein, indicates the presence of nanolime ($Ca(OH)_2$, $pH_{E25} > 11$). By comparing the results of the phenolphthalein test with the photographical observations of the wetting front, conclusion can be drawn on possible phase separation between dispersant (in this case ethanol) and nanolime particles during absorption.

The phenolphthalein test was performed on the specimens saturated with nanolime also during the drying process (at 1, 4, 8, 24 and 48h), in order to understand nanolime migration within the material. Drying tests were performed both in atmospheric and in a nitrogen-rich atmosphere, in order to check the relevance of nanolime carbonation during the drying period. A N2 Boy nitrogen gas-supplying device, by Taitec, was used to create a nitrogen-rich atmosphere within a glass desiccator, where treated specimens were stored.

Microstructural observations

AFM

A TT-AFM device was used to characterize E25 samples; the aim of this analysis was to verify the morphology of the nanoparticles and possible aggregation phenomena, that can affect the transport of nanolime. Nanolime was diluted in its pure ethanol and after several trials a dilution of 1:100 (in volume, that is a concentration of 0.25 g/l of nano-$Ca(OH)_2$ in ethanol) was considered as suitable for AFM analysis. An amount of 5?l was dropped with a micropipette on the freshly cleaved mica substrate (sample holder). Images were aquired in vibration using silicon tips (Brucker model NCHV) and both topographic and phase images were processed. The equipment allows a measurement of the surface topography with a high precision up to nanometric scale.

Optical Microscopy

The drying surface and the cross section of the specimens treated with nanolime were observed with a stereomicroscope Zeiss Stemi SV 11. Images were recorded with a Zeiss AxioCam MRc5 digital microscopy camera. The AxioVision 4.8 software and its interactive measurement tools were used to record and analyse the specimens.

SEM-EDS

The cross-section of the specimens treated with nanolime were studied by SEM-EDS; the equipment (Nova NanoSEM 650, by FEI) is coupled with a low vacuum solid-state detector BSED (GAD) which allows high resolution imaging (up to 1,4 nm) and a high flexibility of the working conditions (1 to 30kV). Samples were collected, at the end of the drying, in the most representative spots (top, middle, bottom) of both specimens types (*TA* and *TB*), as seen in Figure 2.

III. Results

Nanolime characterization by AFM

The observation of E25 by AFM clarifies the particle size of nanolime and aggregation phenomena in the dried phase. Figure 3a shows a heterogeneous distribution of nanolime and a high polidispersivity of the nanoparticle aggregates (with different size and shape); the size of these clusters range from few nanometers to more than 10 μm. Figure 3b and 3c show that clusters are formed by nano (30-100 nm) and sub-micrometric(up to 400 nm) lime particles; the hexagonal plate-like shape, typically observed for these type of nanoparticle (Salvadori, 2001), is possibly deformed by dragging effect originated by the weak absorption of the lime nanoparticle on the mica sample holder (Ambrosi, 2001), and /or to the fraction exerter by the scanning of the AFM tip.

Lime nanoparticles, when the alcoholic solvent has completely evaporated, tend then to form clusters; these aggregation phenomena are an important factor that can affect the deposition of nanolime clusters within the treated material.

When considering the liquid phase (nanoparticle dispersed in the alcoholic solvent), diffuse electrical double layer repulsive interactions would prevent nanoparticle aggregation, at least in diluted dispersions (Rodriguez-Navarro, 2005). Furthermore the low dielectric constant of a low-polarity solvent as ethanol can guarantee a stable dispersion. However lime nanoparticles tend spontaneously to aggregate and attractive Van der Waals forces will keep particles attached once agglomeration has taken place. As argued by Chekli (2013), a particle size concentration dependence at nanoparticle concentrations above 0,05 mg/L has to be considered; when nanoparticle concentration is relevant, like in our case (25g/l), the distance between nanoparticles in the sample is reduced; this presumably increases the chance of collision between particles and hence, their aggregation.

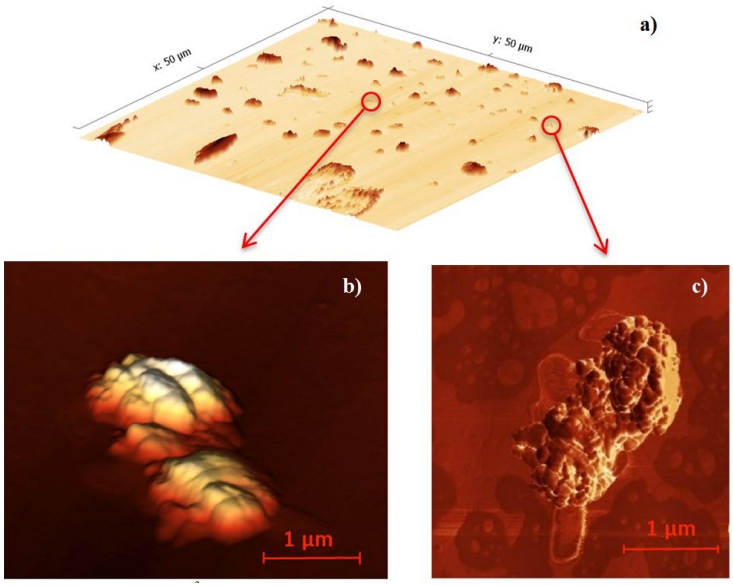

Figure 3: a) Topographical view (50x50 µm^2) by AFM of nanolime clusters in the dried phase with different shape and size; zooom on specific spots: a) topography and b) AFM image of two clusters of E25, formed by the aggregation of lime nanoparticle.

Absorption and drying kinetics

Figure 4a shows the capillary absorption curve of water, ethanol and E25. All these liquids saturate the sample in less than 5 minutes, due to the coarse porosity of Maastricht limestone.

When comparing the behaviour of the different liquids, water absorption is faster than ethanol and E25 absorption. Comparing pure ethanol and E25, a slower absorption is measured for E25. This is due to lime nanoparticles (25g/l), which modify the density (and therefore viscosity) and possibly affect the surface tension of the alcoholic solvent; this affects the capillary transport. Duan (2011) points out that nanoparticle agglomeration, that easily takes place as seen in the previous section, can affect the viscosity of the dispersion and therefore the absorption of the dispersion.

When considering the drying behavior (Figure 4b), the evaporation rate of water is much slower (up to 7 days for complete drying) than that of ethanol (complete drying in 48-72h) or nanolime (up to 72h). The faster evaporation of ethanol can be easily explained by its lower boiling point (78,37 °C) compared to that of water (≈100 °C). Moreover the superficial tension of water (3 times higher than that of ethanol) can explain the higher water retention within the Maastricht pore network.

In the drying curves two stages can be observed. In the 1st stage of drying, called the constant drying period, the drying front is at the surface and the drying rate is constant (Hall, 2012). This first phase ends after 24h in the case of the alcoholic solution (EtOH and E25), while for water it is approximately at 96h. In the 2nd stage of drying, called the falling drying rate period and identified by the change in the slope of the drying curve, the liquid content can no longer support the demands of the evaporation flux. In this stage transport occurs in the vapor phase; thus lime nanoparticles cannot physically take part in the process and are deposited in the material before the end of the 1st stage. It is thus important to observe the deposition of nanolime at 24h, which corresponds to the end of the 1st stage.

By comparing the drying curves of ethanol and nanolime, a slight delay in the drying of the material is observed in the case of E25. Nanolime does not hinder significantly the drying kinetic but a partial occlusion of the pores, caused by the formation of a nanolime layer during drying, could have delayed the evaporation of the solvent.

Phenolphthalein test

Phenolphthalein test was performed as described in section 2.4, immediately after complete saturation of the specimens with nanolime at standard conditions in air (50% RH, 20oC) and in a nitrogen-rich atmosphere. Nanolime has penetrated the whole depth of the specimen (40 mm), as shown in figure 5a. No accumulation of nanolime at the absorption surface is macroscopically visible immediately after specimen imbibition.

By analysing the specimens stored in a nitrogen-rich atmosphere, it is observed that nanolime is stable and homogeneously distributed within the cross section during the first 8 h of drying (Figure 5b,c). At 24 h, a remarkable amount of nanolime is visible nearby the drying surface, whereas just traces are detected in the outer 10 mm beneath the

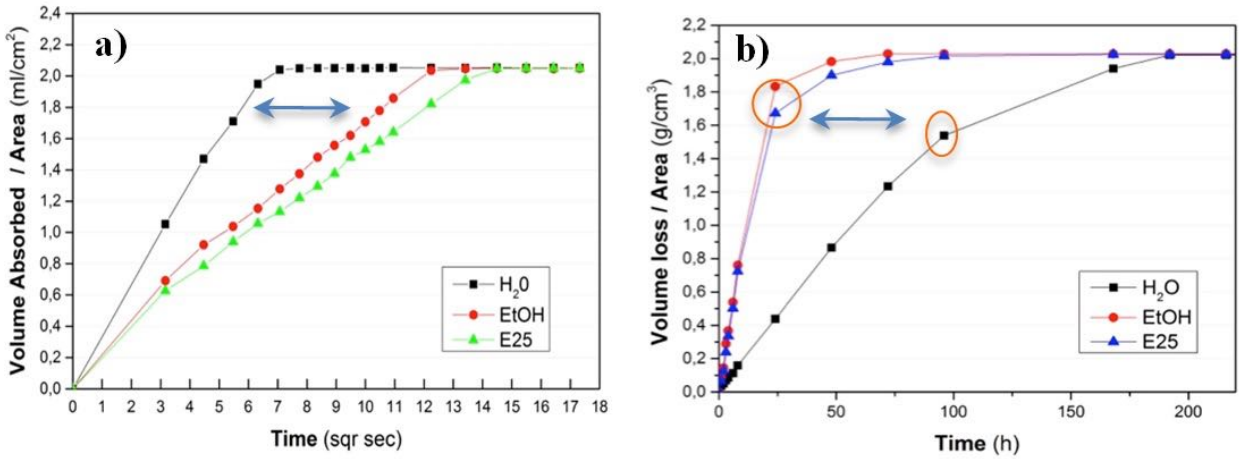

Figure 4: a) Volume comparison of the capillarity wetting curve of water, ethanol and E25; b) Capillarity drying curve in volume of H_2O, EtOH and E25; the red circles indicate the critical liquid content and the end of the first step of drying.

drying surface (Figure 5d). Further microscopical details are presented in the next section.

Microstructural observations by optical microscopy

In order to clarify nanolime transport and deposition within limestone pores network, specimen type TA and TB (described in section 2.3) were characterized by optical microscopy.

In Figure 6 stereomicroscope microphotographs of the cross sections of specimens TA and TB, observed after complete drying (≈72h), are shown. In both cases nanolime accumulates at 0,5-0,7 mm beneath the drying surface. No deposition of nanolime can be identified at the absorption surface of TB.

Observations on specimen TB clarify that nanolime penetrates in the material without any accumulation at the absortion surface during the absorption phase. No phase separation between the particles and the solvent is observed during the absorption process in this stone.

At the same time, traces of nanolime are observed in depth in both specimens, as visible in Figure 7a and 7b. Nanoparticle tends to aggregate. Reduced amount of nanolime are indeed visible in the entire section of both specimens.

The specimens analyzed in section 3.3 (phenolphthalein test) were observed more in detail by optical microcopy (Figure 8a,b); no white deposition was macroscopically identified on the dying surface, but nanolime formed a thin layer beneath the drying surface (at 0,5 mm in depth, Figure 8a,b). The solvent, by evaporating, flows in the direction of the drying surface and nanoparticles partially migrate with the solvent, depositing just beneath the drying surface. This accumulation of nanolime is remarkable at the complete saturation of the solvent (48-72h); this evidence can confirm that nanolime is gradually moving back to the surface with its solvent during drying.

Although most of the nanolime is accumulated just beneath the drying surface, small and heterogeneously distributed amounts of nanolime particles are also observed in depth (20 to 40 mm).

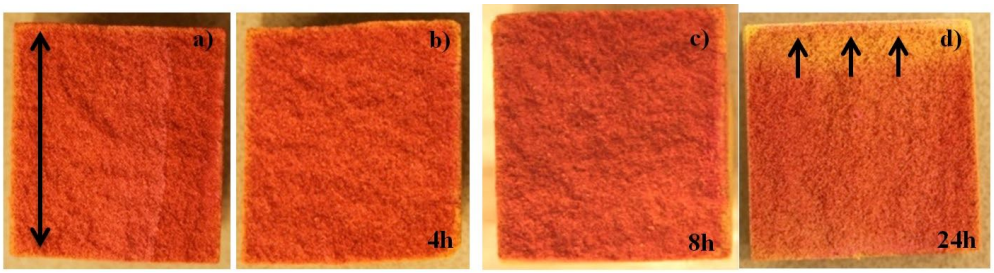

Figure 5: Pictures of the phenolphthalein test performed on the cross sections of specimens treated with E25 (and observed a) immediately after saturation (in air at 50% RH, T=20 °C), with complete saturation of the specimen (arrow); specimens were then stored in a N_2 chamber and observed at b) 4h, c) 8h and d) 24h during drying (each cross section has been obtained by breaking the specimen at the given time and drying surface is on the top of the specimen); a layer of nanolime is visible at 0,5 mm beneath the drying surface (arrows).

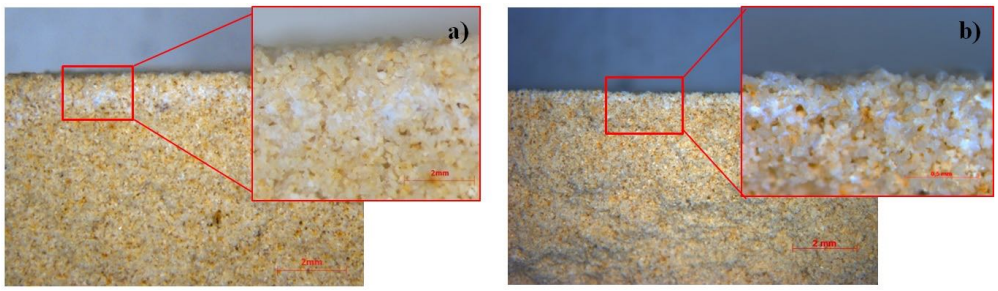

Figure 6: Microphotographs of the limestone cross section in proximity of the drying surface of a) TA and b) TB; in both cases nanolime is accumulated in a thin layer near the drying surface.

Microstructural observations by SEM-EDS

Microstructural observations and microanalyses were performed by SEM-EDS in order to further study the deposition of nanolime within limestone. The cross sections of specimens TA and TB were observed. In both cases, samples were collected from the middle of the specimen, and at the absorption/drying surfaces (Figure 2).

The SEM observations of specimen TA show a significant deposition of nanolime at 0,5 mm beneath the drying surface (Figure 9a, 9b); the relative EDS spectra (9c) highlights the presence of large amounts of carbonated nanolime ($CaCO_3$). Nanoparticles have mainly hexagonal plate-like shape and dimension between 30 to 100 nm. Due to random Brownian motion and attractive short-range van der Waals forces, nanoparticles have mainly agglomerate in clusters (Figure 9b). In fact, similar strong aggregation phenomena are reported in literature for particle size of 1-100 nm, resulting in clusters of typical size 0,1-10 μm (Gaurav, 2009).

Significant deposition of nanoparticles is visible up to 10 mm in depth from the absorption/drying surface; the nanolime particles have deposited filling voids and pores. Pores with diameter of 1 to 5 μm are easily filled with the nanoconsolidant.

Next to the accumulation of nanoparticles clusters near the drying surface, local depositions of isolated nanolime particles are visible almost everywhere in the observed specimen section. Deeper in the stone, at 20 mm from the absorption/drying surface, only sporadic deposits of nanolime particles are observed, heterogeneously distributed (Figure 9d, 9e). At 30 to 40 mm in depth from the drying surface, the presence of nanoparticles (Figure 9f, 9g) is very limited.

When considering the particle size of the nanolime deposits in the cross section, it can be observed that the size of the nanoparticle is smaller (30 to 100 nm) at the drying surface than in depth in the material (150 to 300 nm). This suggests that smaller lime nanoparticle are back-transported more easily to the drying surface, meanwhile bigger nanoparticles (70 to 300 nm) deposit preferentially in depth.

The SEM-EDS analysis of specimen TB shows significant nanolime deposition at 0,5 mm beneath the drying surface (Figures 10a, 10b). Nanolime is visible as well at 10 mm in depth; nanolime deposition is decreasing gradually with depth, with local clusters visible up to 20-25 mm (Figures 10c, 10d). At 35 to 40 mm in depth, in proximity of the absorption surface, some sporadic accumulations of nanoparticles are locally visible (Figure 10e). Nanoparticles have in some cases a tetragonal morphology (Figure 10f), which is typically attributed to aragonite, a thermodynamically unstable polymorph of calcium carbonate.

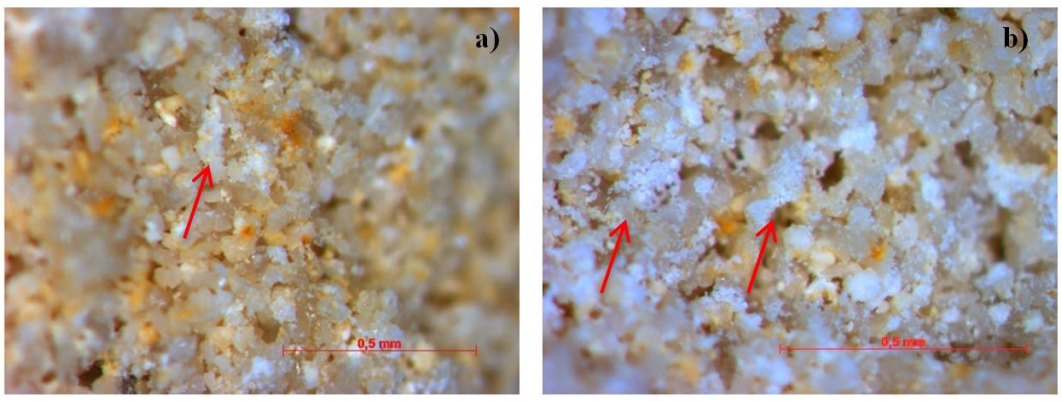

Figure 7: Microphotographs of the limestone cross section: a) traces of nanolime at 20 mm in depth in specimen TA; b) reduced amount of nanolime at 25 mm in depth in specimen TB.

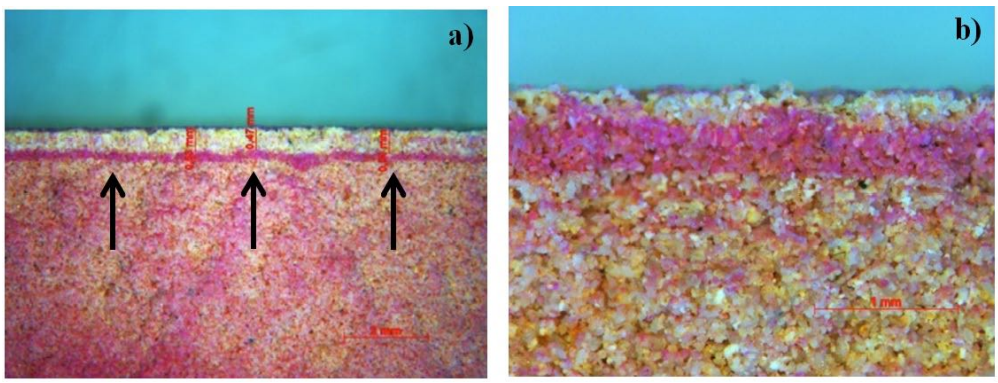

Figure 8: Microphotographs of specimens treated with E25, stored in a nitrogen-rich atmosphere and observed at a) 24h and b) after complete drying (48 to 72h) in a N2 rich atmosphere. A layer of nanolime is visible at 0,5 mm in depth in the drying surface.

These observations demonstrate that the accumulation of nanoparticles, observed at the absorption surface in specimen TA, is not due to reduced penetration and accumulation of the nanoparticles at the absorption surface during absorption, but to migration together with the solvent during the drying phase. These results definitely confirm the observations carried out with phenolphthalein, showing migration of the nanoparticles during drying.

As observed in TA, also in the case of TB the size of nanoparticle is smaller (30 to 60 nm) at the drying surface and considerably larger (70 to 300 nm) in depth.

IV. Conclusion

This paper clarifies the transport of nanolime within Maastricht limestone, a highly porous calcareous material. The results show that a colloidal dispersion of lime nanoparticles in ethanol (CaloSil E25) can easily penetrate in depth in this material without any accumulation at the absorption surface during the absorption phase. Nano and submicron particles (up to 400 nm) can widely fit in the limestone porosity (mean pore size of 35 ?μ). However it appears that accumulation just underneath the surface occurs during drying, when the solvent moves back to the drying surface, depositing an important part of the nanolime particles.

It was observed that the size of the nanoparticles

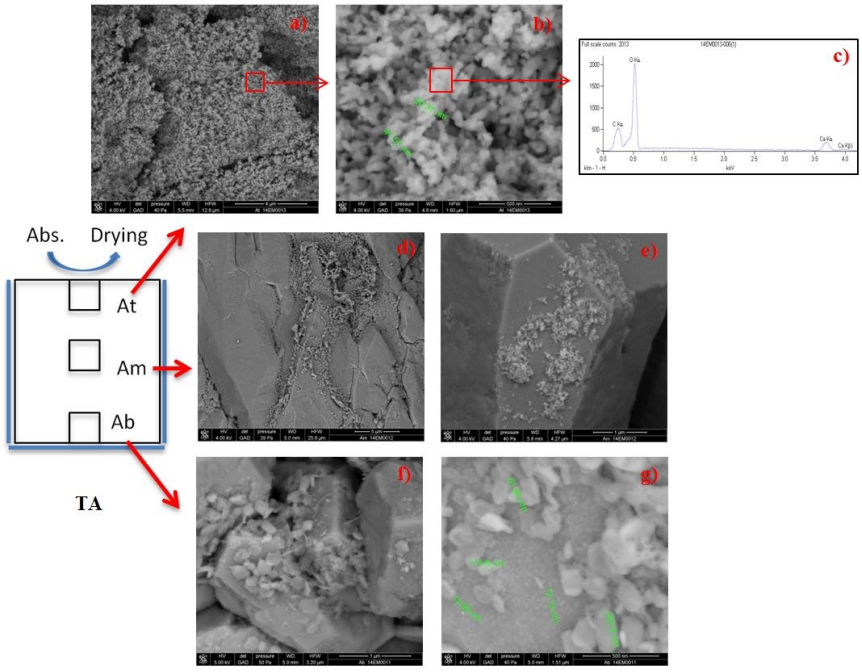

Figure 9: SEM microphotographs of specimen TA at different depths in the cross section (from the drying surface); analysis of sample At at a) 0,5 mm and b) 1,7 mm and c) its relative EDS spectra; analysis of sample Am at d) 20 mm and e) 22 mm; analysis of sample Ab at f) 30 mm and g) 35 mm in depth.

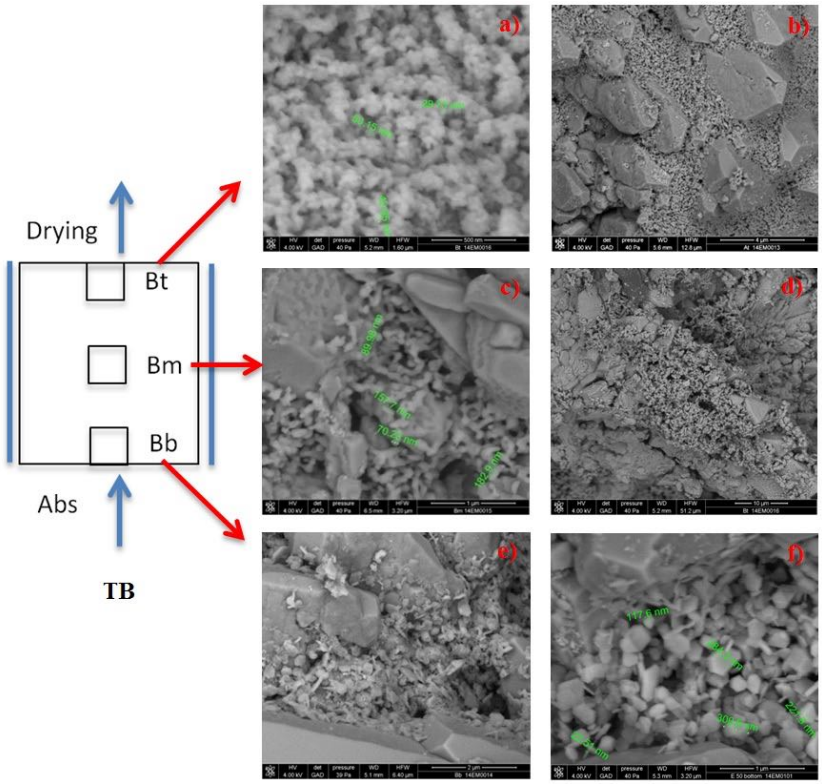

Figure 10: SEM microphotographs of specimen TB at different depths in the cross section (from the drying surface); analysis of sample Bt at a) 0,5 mm and b) 1 mm, with a remarkable accumulation of nanolime; analysis of sample Bm at d) 20 mm and e) 22 mm, with sporadic amounts of nanolime; analysis of sample Bb at f) 32 mm and g) 35 mm, where some lime nanoparticle clusters are visible.

determine the location of their deposition in the stone: smaller lime nanoparticle (30 to 60 nm) much easily migrate back during drying and precipitate in clusters in the proximity of the drying surface, whereas some of the bigger nanoparticles (70 to 400 nm) deposit in depth,

Because of the fast absorption of this coarse porous stone, phase separation between solvent and nanoparticles does hardly take place during absorption; only a small amount of nanoparticles, generally those of large size, is deposited in depth in the material. Aggregation phenomena, which take place in the dispersion mostly due to Brownian motions, favour the formation of clusters; Van der Waals forces keep nanoparticles attached. Anyway these weak bonding phenomena do not guarantee a significant deposition of nanolime in depth in the material.

Besides, the dense nanolime layer (accumulated beneath the drying surface) limits the consolidation effect in depth and the penetration of successive consolidant applications.

These results suggest that in order to improve nanolime precipitation in depth, the transport and deposition mechanism of nanolime should be modified.

A more homogeneous nanoparticles distribution in depth might be obtained by modifying the properties of the solvents. A solvent with slower drying rate and higher dielectric constant might be used to favor nanoparticle/solvent phase separation and induce nanoparticle deposition in depth.

Next to solvent modification, the optimization of improved application strategies might help favoring nanolime precipitation in depth. Research is ongoing to verify these possibilities.

Acknowledgement

Special thanks go to prof. Jorge Caldeira (FCT-UNL, Lisbon) for support in AFM analysis and to Willem Duvalois and Timo Nijland for SEM-EDS analysis

References

Ambrosi, M., Dei, L., Giorgi, R., Neto, C., & Baglioni, P. (2001): "Colloidal particles of $Ca(OH)_2$: properties and applications to restoration of frescoes." *Langmuir*, *17*(14): 4251-4255.

Baglioni, P., Chelazzi, D., Giorgi, R., Poggi, G. (2013): "Colloid and Materials Science for the Conservation of Cultural Heritage: Cleaning, Consolidation, and Deacidification." *Langmuir*, 29: 5110?5122.

Borsoi, G., Tavares, M., Veiga, R., Santos Silva, A. (2012): "Microstructural Characterization of Consolidant Products for Historical Renders: An Innovative Nanostructured Lime Dispersion and a More Traditional Ethyl Silicate Limewater Solution." *Microscopy & Microanalysis*, 18:1181-1189.

Costa, D., Delgado Rodrigues, J., (2012): "Consolidation of a porous limestone with nanolime." In proceeding of *12th Int. Congress on Deterioration and Conservation of Stone*, Columbia University, New York, 22-26 October 2012.

Campbell, A., Hamilton, A., Stratford, T., Modestou, S., Ioannou, I. (2011): "Calcium Hydroxide Nanoparticles for Limestone Conservation: Imbibition and Adhesion." In *Symposium Adhesive and Consolidants for Conservation: Research and Applications*, ICC, Ottawa, Canada, 17-21 October 2011.

Chekli, L., Phuntsho, S., Kandasamy, J., Shon, H. (2013): "Assessing the aggregation behaviour of iron oxide nanoparticles under relevant environmental conditions using a multi-method approach." In Conference Nanotech 2013, Washington DC, Volume: 1.

Doehne, E., Price, C.A. (2010): "Stone Conservation. An Overview of Current Research, Research in Conservation." 2nd edition, The Getty Conservation Institute, Los Angeles.

Dreesen, R., Dusar, M. (2004): "Historical building stones in the province of Limburg (NE Belgium): role of petrography in provenance and durability assessment." Materials Characterization, 53: 273-287.

Duan, F., Kwek, D., Crivoi, A. (2011): "Viscosity affected by nanoparticle aggregation in Al_2O_3-water nanofluids." *Nanoscale Research Letters*, 2011, 6:248.

Dubelaar, C.W., Dusar, M., Dreesen, R., Felder, W.M., Nijland, T.G. (2006): "Maastricht limestone: a regional significant building stone in Belgium and the Netherlands. Extremely weak, yet time-resistant." in *Heritage, Weathering and Conservation Conference - HWC 2006*, Madrid, 21-24 June 2006.

EN 13775 (2008): "Natural stone test methods - Determination of water absorption at atmospheric pressure." European Standard, European committee for Standardization (CEN).

Favaro, M., Tomasin, P., Ossola, F. and Vigato, P.A. (2008): "A novel approach to consolidation of historical limestone: the calcium alkoxides." *Applied Organometallic Chemistry*, 22(12): 698-704.

Gaurav, P. (2009): "Understanding nanoparticle aggregation." PhD thesis, Iowa State University.

Ghaffari, E., Koberle, T., Weber, J. (2012): "Methods of polarising microscopy and SEM to assess the performance of nano-lime consolidants in porous solids." In *12th International Congress on the Deterioration and Conservation of Stone*, Columbia University, New York, 22-26 October 2012.

Giorgi, R.; Dei, L.; Baglioni, P. (2000): "A new method for consolidating wall paintings based on dispersions of lime in alcohol." *Studies in Conservation*, 45: 154-161.

Hall, C., Hoff, W.D. (2012): "Water transport in brick, stone and concrete." Spon Press (Taylor & Francis Group), New York.

Hansen, E., Doehne, E., Fidler, J., Larson, J., Martin, B., Matteini, M., Rodrigues-Navarro, C., Sebastian Pardo, E., Price, P., de Tagle, A., Teutonico, J. M., Weiss, N. (2003) "A review of selected inorganic consolidants and protective treatment for porous calcareous materials." *Reviews in Conservation*, 4: 13-25.

Nijland, T.G., Dubelaar, C.W., Tolboom, H.J., Van Hees, R.P.J. (2006): "Building stones from a muddy delta: Native natural stone from the Netherlands." In *Heritage, Weathering and Conservation Conference- HWC 2006*, Madrid, 21-24 June 2006.

Rodriguez-Navarro, C., Ruiz-Agudo, E., Ortega-Huertas, M., Hansen, E. (2005): "Nanostructure and irreversible colloidal behavior of Ca(OH)$_2$: implications in cultural heritage conservation." *Langmuir*, *21*(24), 10948-57.

Rodriguez-Navarro (2013): "Alcohol Dispersions of Calcium Hydroxide Nanoparticles for Stone Conservation." *Langmuir*, 29: 11457?11470.

Salvadori, B., Dei, L. (2001): "Synthesis of $CaOH_2$ nanoparticles from diols. " *Langmuir*, 12: 2371-2374.

Teutonico, J. M., Charola, A. E., De Witte, E., Grassegger, G., Koestler, R. J., Laurenzi Tabasso, M., Sasse, H. R., Snethlage, R. (1997): "Group report: How can we ensure the responsible and effective use of treatments (cleaning, consolidation, pro- tection)?" In *Saving Our Architectural Heritage: The Conservation of Historic Stone Structures; Dahlem Workshop on Saving Our Architectural Heritage, The Conservation of Historic Stone Structures,* Berlin, 3-8 March 1996, ed. N. S. Baer and R. Snethlage, 293-313.

Toniolo, L; Paradisi, A; Goidanich, S; Pennati, G. (2010): "Mechanical behavior of lime based mortars after surface consolidation". *Construction and Building Materials*, 25 (4): 1553-1559. Van Hees, R., Nijland, T. (2009): "Assessment of the state of conservation of a Middle Neolithic flint mine in Maastricht limestone". *Heron*, Vol. 54, No. 4.

Van Hees, R.P.J., Lubelli, B., Nijland, T., Bernardi, A. (2014): "Compatibility and performance criteria for nano-lime consolidants". In proceedings of *9th International Symposium on the Conservation of Monuments in the Mediterranean Basin - Monubasin 2014* , Ankara, Turkey, 3-5 June.

Ziegenbalg, G., Brummer, K., Pianski, J. (2010): "Nano-Lime - a new material for the consolidation and conservation of historic mortars". In 2nd *Historic Mortars Conference HMC10 and RILEM TC 203-RHM final workhop*, Prague, 22-24 September.